

A Theoretical Framework for DANTE Prepared Pulse Trains: A Novel Approach to Motion Sensitized and Motion Suppressed Quantitative MRI

Linqing Li¹, Karla Miller¹, and Peter Jezzard¹
¹FMRIB, Clinical Neurology Department, University of Oxford, Oxford, United Kingdom

Background: In the present work^[1] it is shown that when DANTE pulse trains shown as Fig.1a are applied, signal from flowing spins is attenuated in a manner largely independent of the flowing spin velocity. We find that the longitudinal magnetization decay of moving spins is dominated by simple progressive saturation as the transverse coherence of the spins is substantially spoiled by motion-induced phase dispersion. The static tissue, conversely, preserves the majority of its transverse coherence despite the gradient fields applied during the DANTE pulse trains. This leads to minimal attenuation of static spins and substantial attenuation of flowing spins. Partially dephased magnetization must also be considered for proper quantification of the static spin magnetization, which itself depends on the number of pulses (N_p) applied in the DANTE pulse train. We derive a full expression by starting from the standard matrix formulation for the steady-state signal^[2] and generalize this to the transient magnetization^[3] and an arbitrary starting magnetization. We then derive a more intuitive approximation by assuming spoiling of the transverse component (complete spoiling for flowing spins and partial spoiling over ≥ 2 DANTE sub-periods for static spins). This approximation is used to quantify the static and flowing spin signals.

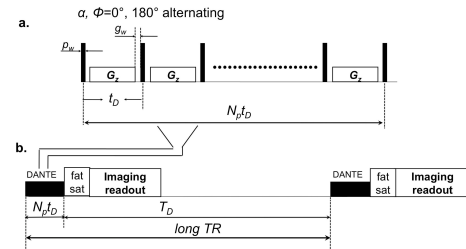


Fig. 1. DANTE multislice interleaved acquisition

comparing analytical solutions and numerical Bloch equation simulations with experimental observations in phantoms and *in vivo*. To understand the mechanism easily, we only consider here the situation with long T_D and a single DANTE module and imaging readout for each TR (the case of short T_D and its application to fast multislice 2D imaging is addressed in a companion abstract).

Methods: The proposed DANTE-BB imaging sequence is shown in Fig. 1, indicating both the DANTE preparation module itself, as well as the proposed method for embedding it within an imaging readout method, such as a TSE sequence. N_p is the number of pulses applied in the DANTE module. T_D in Fig. 1b represents the inter-DANTE module delay time, which is deliberately set to a large value so that longitudinal magnetization largely recovers before a subsequent DANTE module is applied. Assuming spoiled transverse magnetization after each DANTE pulse, the longitudinal magnetization can be treated as an effective longitudinal decay (Eqn. 1), with different apparent T_1 times for moving and static spins (Eqns. 2 and 3). For static spins, we make the simplifying assumption that existing transverse magnetization may contribute to the longitudinal magnetization in the following period, but is spoiled in subsequent periods. Although an extreme simplification this approach should provide some insight into the desired time course of the longitudinal magnetization. Eqns. 4 and 5 are the classic equations for fully spoiled steady state and partially spoiled steady state, respectively. In all the equations, $E_{1,m}^{t_D} = \exp(-t_D/T_{1,m})$, $E_{1,s}^{t_D} = \exp(-t_D/T_{1,s})$ and $E_{2,s}^{t_D} = \exp(-t_D/T_{2,s})$. $M_{0,m}$ and $M_{0,s}$ are the equilibrium magnetizations of the moving and static spins, respectively; $T_{1,m}$, $T_{1,s}$ and $T_{2,s}$ are the T_1 values of the moving and static spins and T_2 of the static spins; α is the small flip angle of the individual pulses in the DANTE pulse train; and t_D ($t_D \ll T_{1,m}$, $T_{1,s}$ and $T_{2,s}$) is the time interval between the DANTE pulses.

$$M_{z,l}^{t_D}(N_p) = (E_{1,app,l})^{N_p} (M_{0,l} - M_{zss,l}) + M_{zss,l} \quad (1)$$

where $l=m$ (moving spin) or s (static spin). When $l=m$, $E_{1,app,m} = \cos \alpha E_{1,m}^{t_D}$ ---(2) and when $l=s$, then

$$E_{1,app,s} = \sqrt{E_{1,s}^{t_D} E_{2,s}^{t_D} \cos \theta \sin^2 \alpha + (E_{1,s}^{t_D})^2 \cos^2 \alpha} \quad (3)$$

$$M_{zss,m} = M_{0,m} \frac{1 - E_{1,m}^{t_D}}{1 - E_{1,m}^{t_D} \cos \alpha} \quad (4)$$

$$M_{zss,s} = q [(\cos \alpha (1 - E_{2,s}^{t_D} \cos \theta) + E_{2,s}^{t_D} (E_{1,s}^{t_D} - \cos \theta))] \quad (5) \quad [4]$$

$$q = \frac{M_{0,s} (1 - E_{1,s}^{t_D})}{(1 - E_{1,s}^{t_D} \cos \alpha)(1 - E_{2,s}^{t_D} \cos \theta) - (E_{1,s}^{t_D} - \cos \alpha)(E_{2,s}^{t_D} - \cos \theta) E_{2,s}^{t_D}} \quad (6) \quad \theta = \gamma r \cdot \int_0^{t_D} G(t) dt + \gamma t \Delta B(r)$$

Results: *Quantification of moving spins and static spins in phantoms and in-vivo:* The images shown in Fig. 2 were acquired by setting the number of pulses (N_p) and time interval between pulses of DANTE (t_D) to 150 and 1ms, respectively. With a long $TR=2s$, four different DANTE pulse train flip angles of 0° , 4° , 6° and 8° were assessed. It is clear that at a flip angle of 8° the flowing signal has disappeared without discernable change to the static water signal. The area inside the residual water circle for the $FA=8^\circ$ data was chosen as the 'flow' ROI, shown magnified in the upper right corner. The quantified attenuation of static and moving spin is also displayed in Fig. 2. Additional values for the number of DANTE pulses within each train ($N_p = 150, 300, 600$) were selected for these flow-crushing experiments. Theoretical curves, calculated via Eqns. 1 and 2, agree well with measured results. *In-vivo*, a DANTE flip angle of 5° was kept constant for all acquisitions while N_p values of 0, 2, 200, 400, 800 and 1600 were used. Only images of the vessels in the neck with $N_p=2$ and 1600 are shown in Fig. 3. The muscle signal $M_{zss,s}=76\%$ contained in ROI '3', ($N_p=1600$ from Fig. 3) was used with a precession angle $\theta=28^\circ$ calculated by employing the classic steady state Eqn. 5. This average precession angle was then inserted into the Bloch equation simulation to yield the solid curve in Fig. 3, and into Eqns. 1 and 3 to yield the simple decay curve shown by the dotted line. Both curves agree with the measured signal intensity of muscle during this non-steady state period of the DANTE train evolution.

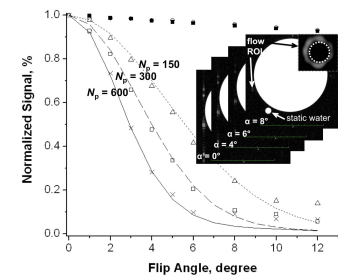


Fig. 2 Moving spins in phantom

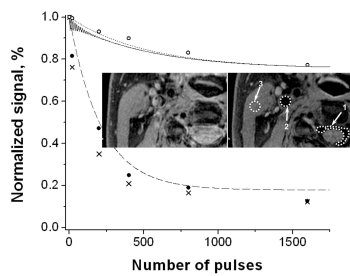


Fig. 3 Static spins *in vivo*

Theoretical curves, calculated via Eqns. 1 and 2, agree well with measured results. *In-vivo*, a DANTE flip angle of 5° was kept constant for all acquisitions while N_p values of 0, 2, 200, 400, 800 and 1600 were used. Only images of the vessels in the neck with $N_p=2$ and 1600 are shown in Fig. 3. The muscle signal $M_{zss,s}=76\%$ contained in ROI '3', ($N_p=1600$ from Fig. 3) was used with a precession angle $\theta=28^\circ$ calculated by employing the classic steady state Eqn. 5. This average precession angle was then inserted into the Bloch equation simulation to yield the solid curve in Fig. 3, and into Eqns. 1 and 3 to yield the simple decay curve shown by the dotted line. Both curves agree with the measured signal intensity of muscle during this non-steady state period of the DANTE train evolution.

Conclusions The analytical framework of moving and static spins agrees with the numerical Bloch equation simulations and experimental observations in phantoms and *in vivo*.

Acknowledgements We thank the NIHR Oxford Biomedical Research Centre for grant funding

References [1] Li L, Miller K and Jezzard P (2011) in revision. [2] Carr H, Phys Rev, 112:1693-1701. [3] Hargreaves BA, (2001), MRM, 46: 149-158. [4] Freeman R, Hill HDW (1971) J. Magn. Reson. 4: 366-383.